High-Resolution Shallow Structure Constrained by ambient noise S-wave tomography using dense linear arrays—a case study in northern Hong Kong

Guoxu Chen, Tao Xie, Zhiqian Liu, Liang Lyu, Hansong Pang, Boyang Su, Shupeng Chai, Andy Y. F. Leung, Yiqing Ni & Qi Zhao
The Hong Kong Polytechnic University, Hong Kong
Dennis C.S. Lau
AtkinsRéalis Asia Limited, Hong Kong

doi: https://doi.org/10.21467/proceedings.7.7.18

ABSTRACT

Conducting shallow structure tomography in Hong Kong is of great significance for engineering construction, urban underground space utilization, and geological disaster prevention. In this study, we deployed a linear array of 48 node seismometers at a construction site in northern Hong Kong and collected ambient noise data for about 2 days. The effects of different stacking durations and stacking methods on the noise cross-correlation function (NCF) were tested, indicating that the signal-to-noise ratio of NCF can be effectively improved by considering weighted methods during short-time stacking. We used the passive source-based multi-channel analysis of surface wave method (MASW) to extract the Rayleigh wave dispersion curve and inverted it to obtain the two-dimensional S-wave profile of the test site. Our results demonstrate that shallow S-wave tomography based on ambient noise data can quickly, safely and non-invasively constrain shallow structures, showing great potential for underground engineering applications.

1 INTRODUCTION

Reliable detection of shallow surface structures can provide important priori guidance for practical applications such as urban underground space development, geological disaster prevention, and engineering construction. Especially in Hong Kong, the vigorous promotion of the Northern Metropolis Development Strategy requires effective investigation of shallow structures in northern Hong Kong to ensure safe and efficient construction. In addition to the igneous rocks（including granite and volcanic rocks) formed during the large-scale volcanic eruptions of the Mesozoic era, the northeastern New Territories also feature extensive sedimentary rocks, which account for approximately 15% of land surface of Hong Kong (Sewell, 2000). This contributes to the complex geological settings of the Northern Metropolis, distinguishing it from other regions of Hong Kong. The presence of sedimentary rocks provides the necessary geological conditions for the development of karst cavity, and significant karst morphology has already been discovered in the Yuen Long area (Chan et al., 1994). Therefore, it is necessary to investigate and assess the shallow geological conditions of the Northern Metropolis using appropriate methods.

Seismic tomography is an effective method for multi-scale detection of underground structures (Aki et al., 1977; Park et al., 1999; Shapiro et al., 2005; Virieux & Operto, 2009). Seismic wave signals generated by natural earthquakes or artificial sources carry valuable information about the medium through which they pass. Through appropriate mathematical and physical modeling, the physical parameters of the underground medium (such as P-wave/S-wave velocity, attenuation, etc.) can be constrained by inversion to image two-dimensional or three-dimensional imaging of underground structures. At the engineering scale, shallow structures tens to hundreds of meters underground are particularly important because they are closely related to human activities and urban development. Commonly used shallow structure detection methods can be divided into body wave-based and surface wave-based methods. The body wave data collected based on active sources can be used for seismic

Proceedings DOI: 10.21467/proceedings.7.7; Series: AIJR Proceedings; ISSN: 2582-3922; ISBN: 978-81-989164-3-3

reflection/refraction imaging and is widely used in geological surveys. On the other hand, the surface wave method is based on the inversion of surface wave signals collected by active or passive sources. The lateral resolution in shallow layers is relatively high. Besides, the tomographic S-wave velocity can be used to effectively evaluate site characterization (Foti et al., 2011). Therefore, it has been widely used in engineering practice. The traditional active source high-frequency surface wave method uses hammer, vibroseis truck, etc. to stimulate active sources to collect surface wave signals, and extracts the phase velocity dispersion curve for inversion through methods such as multi-channel analysis surface wave (MASW). This type of active source method offers high resolution in shallow part due to the high frequency of the data used (several Hz to tens of Hz), but it also faces the limitations of high equipment and labour costs and limited imaging depth.

Ambient noise tomography has developed rapidly in the past 20 years and has been successfully applied in the imaging of crust-mantle structures and shallow surface structures (Nakata & Snieder, 2012; Shapiro et al., 2005). Under the assumption that the noise source is uniformly distributed and the interior of the study area is homogeneous, previous studies have shown that the Green's function of the wave field can be generated from the cross-correlation function of the station pair (Kästle et al., 2016; Lobkis & Weaver, 2008). Therefore, by long-term stacking of ambient noise data segments, the empirical Green's function (EGF) with one seismometer station as a virtual source and the other station as a receiver can be obtained and used for surface wave tomography. The primary noise source in urban environments is traffic noise (with frequency bands ranging from a few to several tens of Hz). In specific areas, it also includes construction noise (such as from construction sites). Therefore, it is effective to utilize the ambient noise continuously generated by these urban noise sources to conduct shallow subsurface structure tomography. Compared to active source surface wave methods, this approach offers advantages such as lower cost, safety, and greater detection depth, considering that the noise source is generally lower in frequency than the active source. Combining ambient noise tomography with MASW allows for the effective extraction of phase velocity dispersion curves and S-wave imaging without relying on active sources (Cheng et al., 2016; Cheng et al., 2015).

In this study, we investigated the effects of different stacking durations and stacking methods on noise cross-correlation functions (NCFs) based on ambient noise data collected at a construction site. Based on the stacked NCFs, we extracted phase velocity dispersion curves through passive source MASW and inverted them to obtain a 2D S-wave profile of the test site. Our results demonstrate that this method can safely and effectively estimate the S-wave structure of the site, showing great potential for application in engineering construction in Hong Kong.

2 TEST SITE AND DATA COLLECTION

The test field is located at a construction site in Fanling, in the northern region of Hong Kong. For ambient noise data collection in this experiment, we utilized the ANT-1C (5 Hz) vertical component node seismometer manufactured by Earth Pulse Technologies (Wuxi) Co., Ltd. This equipment features an effective frequency range of 0.2 to 1000 Hz, fully covering the surface wave frequency band of interest (1-50 Hz). We deployed a nearly linear array consisting of 48 nodes (labelled sta01 to sta48, increasing from south to north along the survey line) with 2-meter spacing, forming a survey line approximately 94 meters in length (Figure 1b). Each node was set to a sampling rate of 1000 Hz. Besides, alongside the linear array of node seismometers, we have deployed a distributed acoustic sensing (DAS) cable to collect axial strain data (Figure 1c), which will be combined with the data from node seismometers in future studies. Data collection spanned approximately 42 hours, from 6:00 p.m. on March 22, 2025, to 12:00 a.m. on March 24, 2025 (Hong Kong time). There is a nearly parallel road (Ma Tak Road) on the east side of the survey line, where construction vehicles often travel back and forth on weekdays (Figure 1b). Approximately 1.2 km southwest of the survey line lies the East Rail Line (Figure 1a), contributing to the stable ambient noise sources we are aware of. In addition, vibrations that can be sensed by instruments, such as building construction and human activities, will also be recorded.

Proceedings DOI: 10.21467/proceedings.7.7
ISBN: 978-81-989164-3-3

Series: AIJR Proceedings
ISSN: 2582-3922

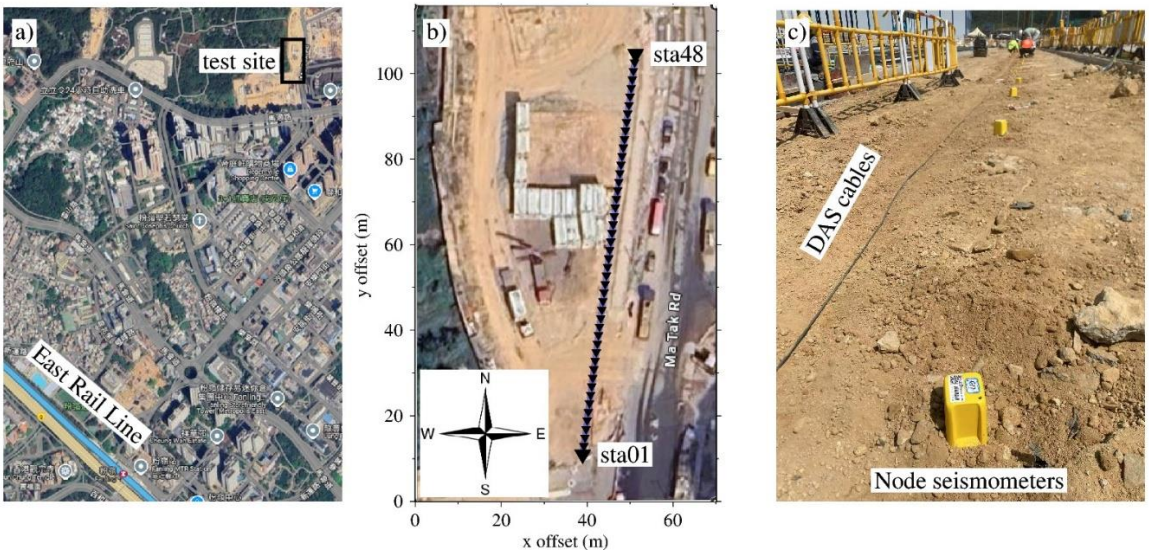

Figure 1: Test site and node seismometers used for data collection.

We can roughly divide the data collection periods into the following three types: daytime on rest days, nighttime on rest days, and daytime on working days. The collected data reveals a distinct day-night pattern in ambient noise signals, closely linked to human activities. Using sta01 as an example, we extracted one-hour segments of data for Power Spectral Density (PSD) analysis for each of these periods (Peterson, 1993). The specific durations are: 0:00 a.m. to 1:00 a.m. on March 23, 2025 for nighttime on rest days (Sunday), 12:00 a.m. to 1:00 p.m. on March 23, 2025 for daytime on rest days, and 9:00 a.m. to 10:00 a.m. on March 24, 2025 for daytime on working days (Monday). Next, we use PSD to estimate the energy distribution of different frequency components of the recorded ambient noise. For each ambient noise time series $s(t)$, the PSD can be calculated by

$$p(\omega) = \frac{1}{T}|U(\omega)|^2, \quad (1)$$

where T is the signal duration and $U(\omega)$ is the Fourier spectrum of $s(t)$, defined by $U(\omega) = \int_{-T/2}^{T/2} s(t)e^{-i\omega t}\mathrm{d}t$.

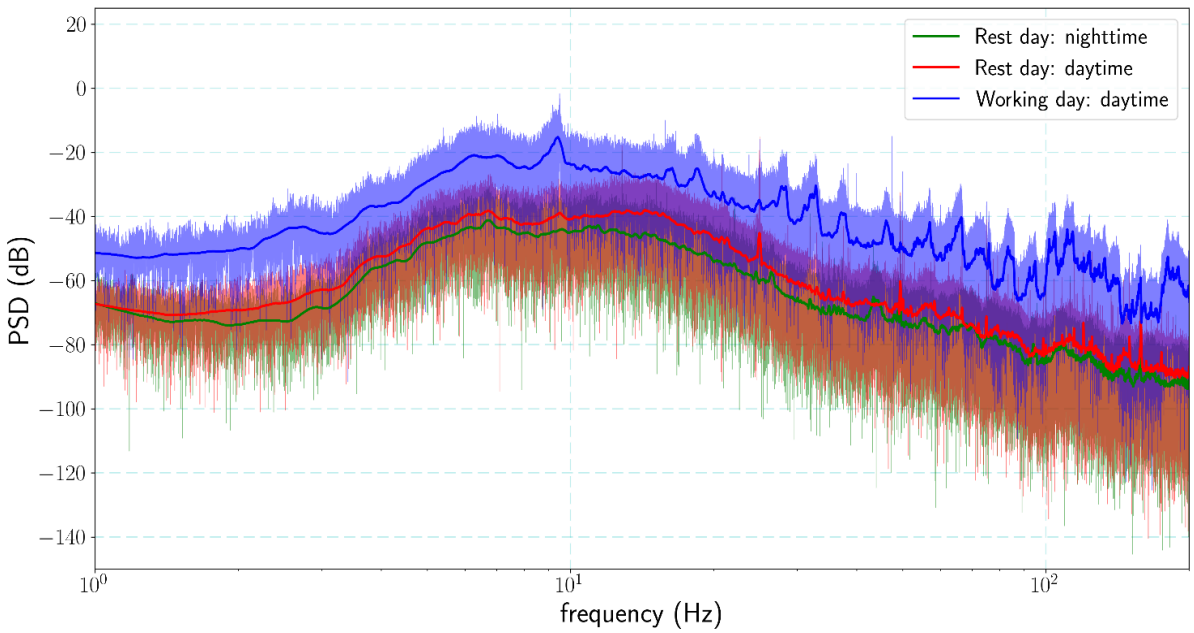

Figure 2: Power spectral density (PSD) of ambient noise signal at different periods.

Figure 2 illustrates the PSD estimates for three time periods. It can be found that in any frequency band, the noise energy during the daytime on working days is significantly higher than that on rest days, indicating that human activities such as traffic transportation and construction substantially enhance the signal energy. Additionally, the noise energy during the daytime is slightly higher than that at nighttime. In the traffic noise frequency band (a few to tens of Hz), the ambient noise records for all three time periods exhibit stronger energy.

3 DATA PROCESSING

3.1 Cross-correlation stacking

The extraction of cross-correlation functions (CCFs) from ambient noise data has advanced significantly over the past two decades, leading to the development of a well-established data processing workflow. For data preprocessing, we primarily follow the methodology outlined by Bensen et al. (2007), which is essential for subsequent cross-correlation stacking to obtain NCFs. For the raw data collected by each node seismometer, the following steps are executed sequentially to prepare the waveform for cross-correlation. Using the one-hour data recorded by sta01 as an example, we first remove the instrument response, mean, and linear trend to obtain the ground motion. The signal is then downsampled to 200 Hz, and a zero-phase second-order Butterworth band-pass filter with corner frequencies of 1-30 Hz is applied to produce the preprocessed waveform (Figure 3a). Next, time domain normalization is applied to the preprocessed waveform to mitigate the influence of irregular instrument noise and non-stationary noise sources near the station. Common time domain normalization techniques include running absolute mean normalization and one-bit normalization. We adopt the latter, which uses a sign function to normalize the time domain signal, due to its simplicity and effectiveness (Figure 3b). Finally, spectral whitening is performed, that is, normalization in the frequency domain, to smooth the noise spectrum and broaden the frequency band of the signal (Figure 3c-d). Figure 3e illustrates the time domain signal obtained by inverse Fourier transform after spectral whitening, which is ready for the next step of time domain cross-correlation.

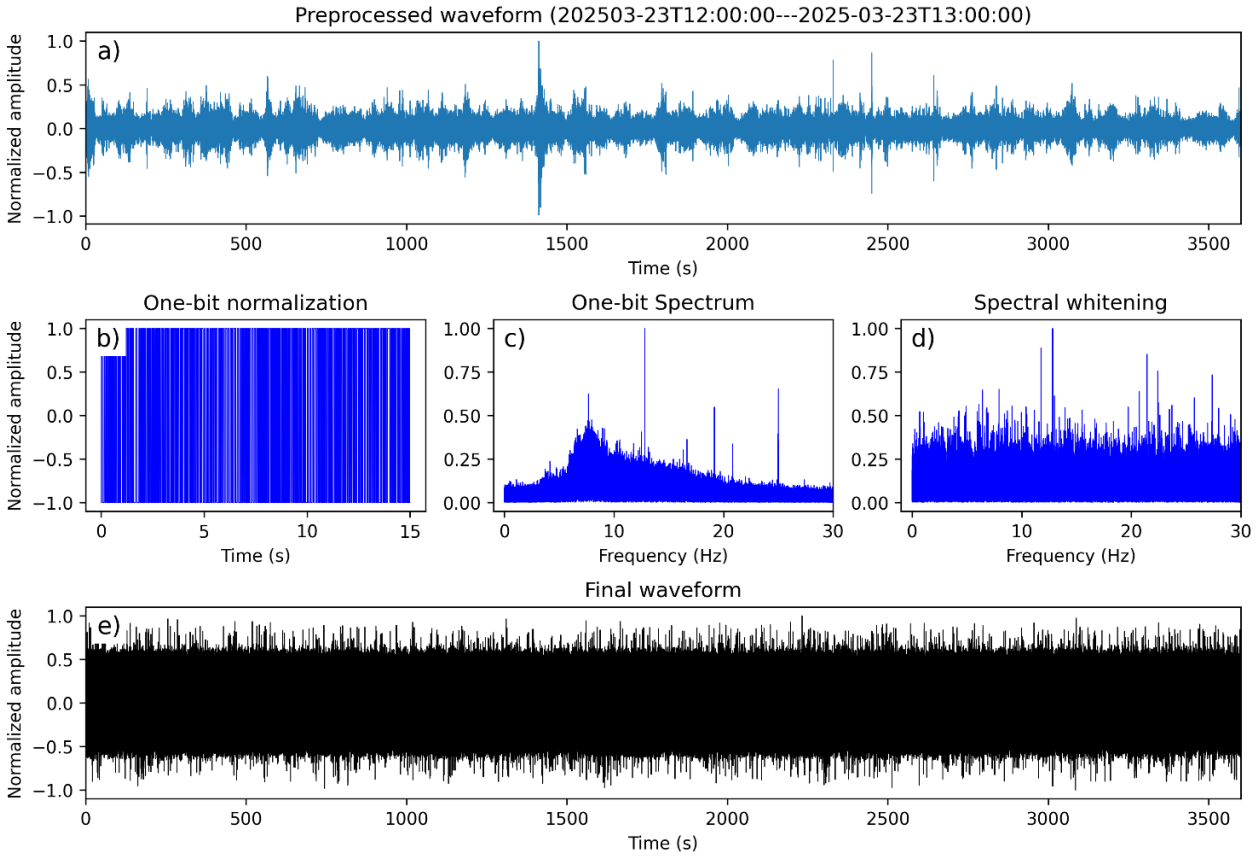

Figure 3: Data processing workflow for a single station.

Proceedings DOI: 10.21467/proceedings.7.7
ISBN: 978-81-989164-3-3

Series: AIJR Proceedings
ISSN: 2582-3922

NCFs are derived by stacking the CCFs of pre-processed waveform segments between station pairs. We evaluated the effects of different stacking durations and stacking methods on NCFs. For each station, we prepared signal lengths of 1 hour (from 2024-03-22T18:00:00Z to 2024-03-22T19:00:00Z) and 42 hours (from 2024-03-22T18:00:00Z to 2024-03-24T12:00:00Z) to test short-time stacking and long-time stacking, respectively. All signals are cut into segments of 2 seconds, resulting in 1,800 segments for short-term stacking and 75,600 segments for long-term stacking to obtain NCFs. We employed four different stacking methods: linear stacking, SNR-weighted stacking, phase-weighted stacking (PWS), and time-frequency domain phase-weighted stacking (tf-PWS), to evaluate the SNR of the generated NCFs. Linear stacking is a traditional approach that obtains NCFs by directly stacking all CCFs together. Typically, surface wave signals with high SNR can generally be obtained through long-time signal stacking. SNR-weighted stacking pre-screens CCFs by setting a threshold, retaining only those CCFs with SNR greater than the given threshold for stacking and rejecting CCFs below the threshold, and using the SNR of CCFs as a weight for signal stacking, thereby effectively improving the signal quality of the NCF (Cheng et al., 2015). PWS is a nonlinear stacking method based on the instantaneous phase. We first calculate the analytical signal $S(t)$ of the seismic signal $s(t)$ by Hilbert transform $S(t) = s(t) + iH\big(s(t)\big) = A(t)e^{i\Phi(t)}$, here $A(t)$ and $\Phi(t)$ are the amplitude and instantaneous phase of the signal, respectively. Then, by calculating the phase coherence of the signal, different weights are assigned to the original linear stacking to improve the SNR of the final signals (Schimmel & Paulssen, 1997). In detail, PWS stacked signals is formulated as

$$g(t) = \frac{1}{N}\sum_{j=1}^{N} s_j(t)\left(\frac{1}{N}\sum_{k=1}^{N} e^{i\Phi_k(t)}\right)^{v}, \quad (1)$$

where N represents the total number of stacked segments, and v is the weight factor. PWS is equivalent to linear stacking if we take $v = 0$. Increasing v enhances the suppression of random noise but may lead to waveform distortion. Here, we follow the common practice of setting $v = 1$. tf-PWS is an extension of PWS (Schimmel et al., 2011) by transforming the signal into the time-frequency domain using the S transform, stacking the waveforms, and then applying the inverse S transform to obtain the final tf-PWS waveform (Schimmel et al., 2011).

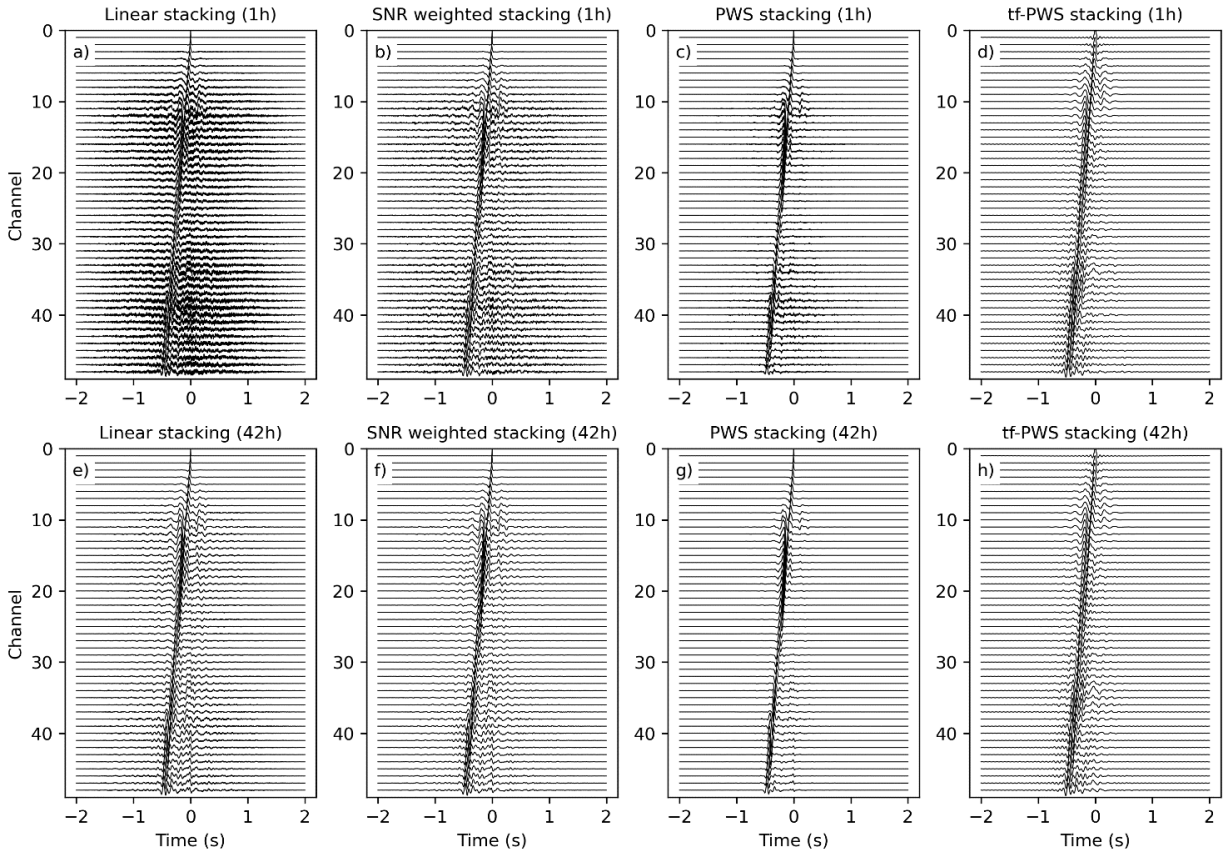

Figure 4: Comparison of the effects of stacking duration and method on NCFs.

Figure 4 illustrates the effects of stacking duration and method on NCFs, obtained by cross-correlating sta01 with all other stations using different stacking methods. We can clearly observe surface wave signals in nearly all stacking results. For short-time stacking (1h), the SNR of NCFs obtained based on linear stacking is slightly lower. Above mentioned weighting methods can all enhance the SNR of NCFs, with the PWS method showing the best improvement (Figure 4a-d). For long-time stacking (42h), almost all stacking methods reveal surface wave signals with high SNR considering that the data collection is long enough (Figure 4e-h). Therefore, SNR weighted method and tf-PWS method have limited improvement in signal quality. However, the improvement of waveform SNR by PWS can still be observed. This illustrates the necessity of weighted stacking when long-term acquisition is difficult to achieve (such as regulatory restrictions on experimental sites). It is worth mentioning that in an ideal situation (noise sources are evenly distributed), stacked NCFs should be symmetric about the origin. Here, regardless of stacking duration, signal energy is predominantly concentrated in the non-causal branch (negative half-axis in the time domain), indicating the presence of stable and uneven noise sources near the test site, particularly in the southern part of the survey line. We speculate that this may be the influence of the East Rail Line. In future studies, waveform beamforming analysis may be used to more accurately study the distribution of regional ambient noise sources.

3.2 Dispersion curve extraction

We employ the multi-channel analysis of surface wave (MASW) method based on the phase shift method (Park et al., 1999; Xia et al., 1999) to extract the Rayleigh surface wave dispersion. In the frequency domain, the phase difference of each channel is calculated according to the phase velocity and distance. The phase-corrected signals from each channel are then stacked to obtain the stacking energy corresponding to a specific frequency and phase velocity. The maximum value of the stacking energy of each frequency in the frequency-phase velocity map is taken as the corresponding phase velocity, thereby forming a dispersion curve. It reflects the S-wave velocity structure below the midpoint of the linear channels used (Cheng et al., 2015).

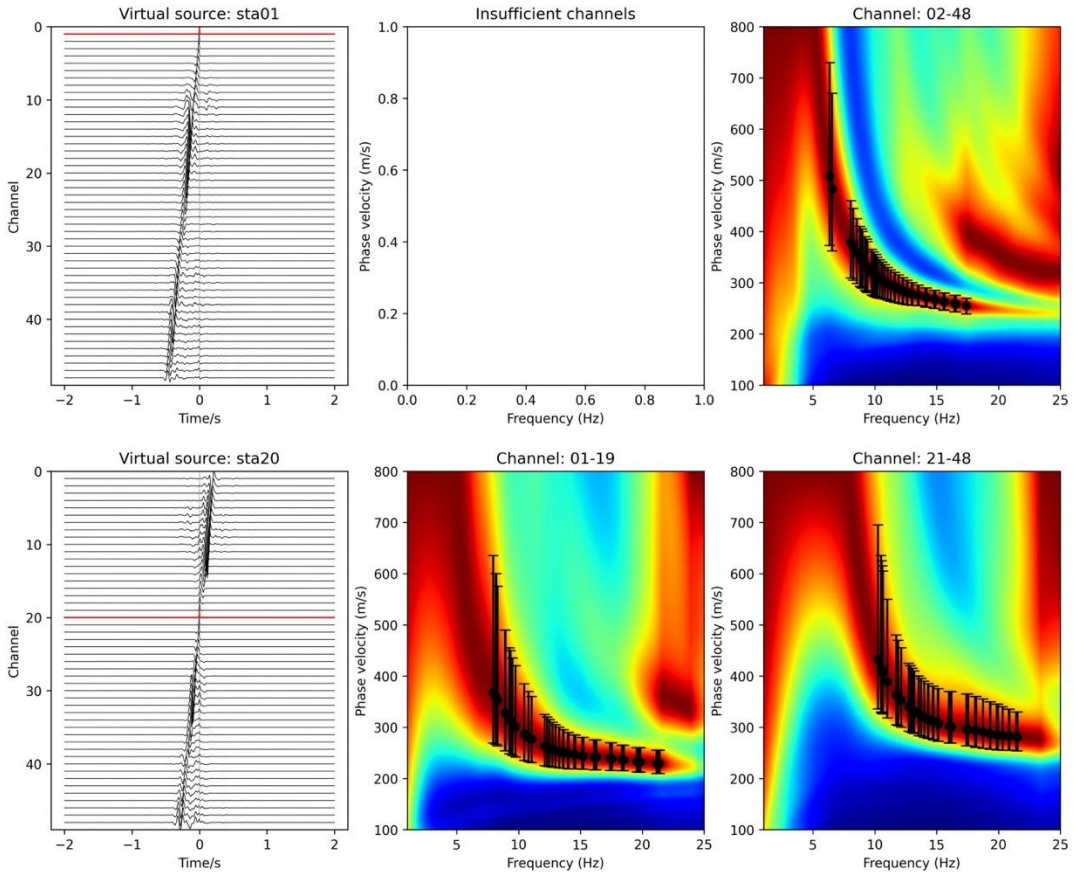

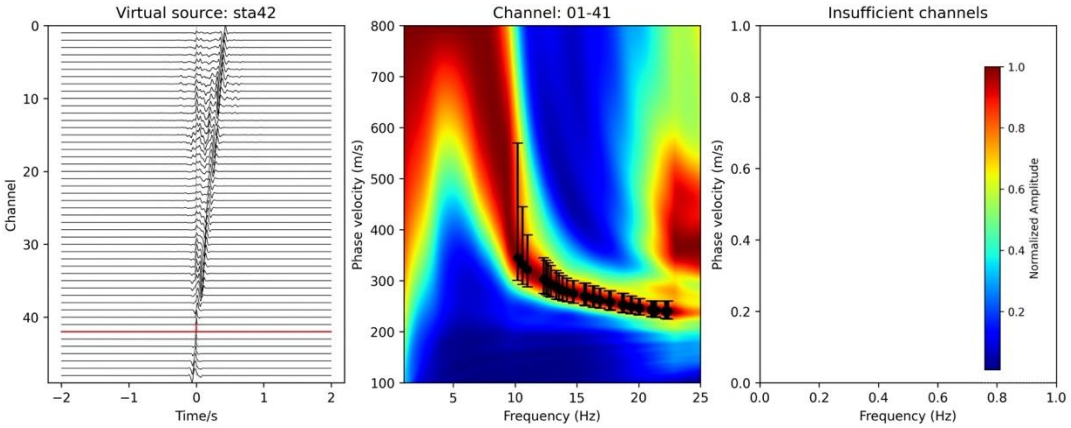

Figure 5：NCFs and corresponding surface wave dispersion spectrum imaging obtained using sta01, sta20, and sta41 as virtual sources

We use bidirectional shot mode to determine the subset of linear arrays used for dispersion curve extraction (Cheng et al., 2015). Specifically, except for sta01 and sta48, each station (virtual source) can be regarded as a bidirectional shot, allowing each virtual source to generate two common virtual source gathers (CVSGs) in addition to those at the two ends. For example, with sta20, the CVSG composed of sta01-sta19 on the left can be used for imaging the midpoint of this subarray, and the CVSG composed of sta21-sta48 on the right is similar. The resolution of the frequency-phase velocity map generally increases with the number of channels. Here, we empirically set the minimum number of channels that a CVSG should contain to 12, meaning that sta13-sta46 are used as bidirectional shots. The remaining stations serve as unidirectional virtual sources. Figure 5 displays the NCFs of the three stations as virtual sources and the dispersion curves extracted based on the phase shift method. Note that sta01 and sta41 are unidirectional virtual sources, which means they can only extract one dispersion curve each. In contrast, sta20 is considered a bidirectional shot, allowing its two subarrays on the left and right sides to be used for extracting dispersion curves separately.

4 SHEAR WAVE VELOCITY INVERSION

For each CVSG, the corresponding surface wave dispersion curve data can be inverted to characterize the one-dimensional S-wave structure at the array midpoint of the CVSG. Considering the total survey line length of about 94 m and the 2 m station spacing, we can approximately determine the structure of the middle part of the total survey line from 14 to 85m. By combining all the one-dimensional velocity models, we can construct a two-dimensional velocity profile, providing a more comprehensive analysis of the subsurface structure.

The inversion of dispersion curves is a typical ill-posed problem with strong nonlinearity and non-uniqueness. The target is to find a locally optimal S-wave velocity model that best fits the observed dispersion data. To achieve this, we utilize the Cooperative Particle Swarm Optimizer (CPSO) heuristic algorithm (Van den Bergh & Engelbrecht, 2004) to search for the best model. The objective function is considered as the root mean square error (RMSE) between the observed data and the synthetic data. Here the synthetic dispersion data is forward-modeled based on the fast delta matrix algorithms developed by Buchen and Ben-Hador (1996) , which can be implemented with open source software packages such as Computer Programs in Seismology (Herrmann, 2013) or disba (Luu, 2021). In addition to being mainly affected by the S-wave velocity, layer thickness, density and P-wave velocity also have an impact on dispersion data. Given the limited length of the linear array, the uncertainty associated with low-frequency data is relatively high (Figure 5). Therefore, we focus on using dispersion data with frequencies greater than 7.5 Hz for inversion, if available. Based on the extracted dispersion curve data, the phase velocity for 7.5 Hz is estimated to be approximately 400-500 m/s, corresponding to a wavelength of about 60 m. According to previous research, the detection depth for surface waves in shallow structure is typically about 0.5-0.67 times its wavelength, which limits the reliable inversion depth to 32 meters. The layer thickness is set to 4 m, which is twice the station spacing. The P-wave velocity and density are estimated by empirical formulas (Brocher, 2005) and are adjusted simultaneously with the update of the S-wave velocity model during the inversion.

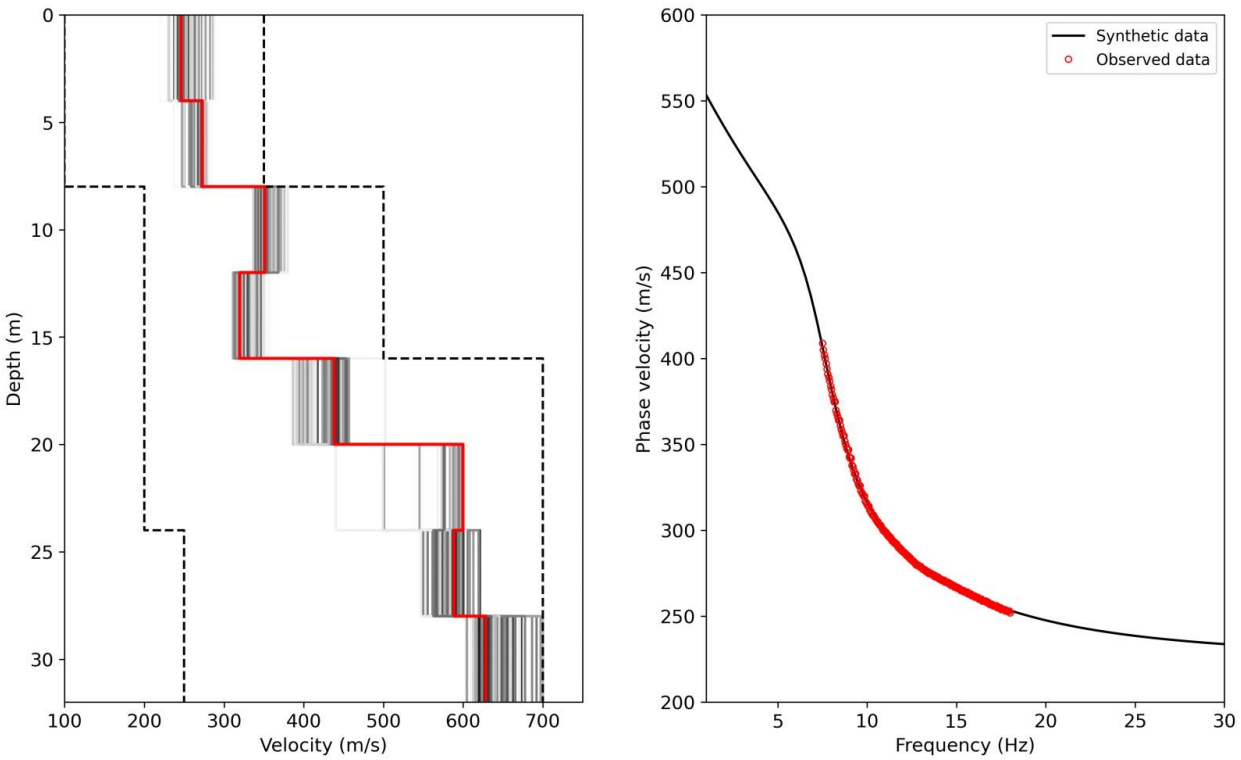

Figure 6: Dispersion curve inversion using sta01 as a virtual source

Figure 6 presents the inversion results of CVSG data (sta02-sta48) using sta01 as the virtual source. As previously mentioned, it reflects the midpoint of CVSG, that is, the one-dimensional S-wave structure located 50 meters from the start of the survey line. The black dashed lines give the upper and lower bounds of the search range for model parameters. Gray lines depict 500 models with the smallest objective function values, while the red line represents the final inversion result. Based on the obtained velocity model, we can calculate the synthetic dispersion curve, and find that it corresponds well to our observed data, which to some extent illustrates the reliability of the inversion. We apply similar processing to all CVSGs to obtain the corresponding one-dimensional S-wave models. The final 2D velocity profile is constructed by the combination of all 1D models (Figure 7). The final model shows significant lateral heterogeneity, especially in the left half of the section, where the dispersion data covers lower frequencies and thus has better constraints on the deeper structure. For the right part, the dispersion data coverage is generally above 10 Hz, and the dispersion data at different inversion points have similar distributions, thus showing a similar structure. In subsequent studies, we will combine core data and active source data for joint analysis to enhance the reliability of the results.

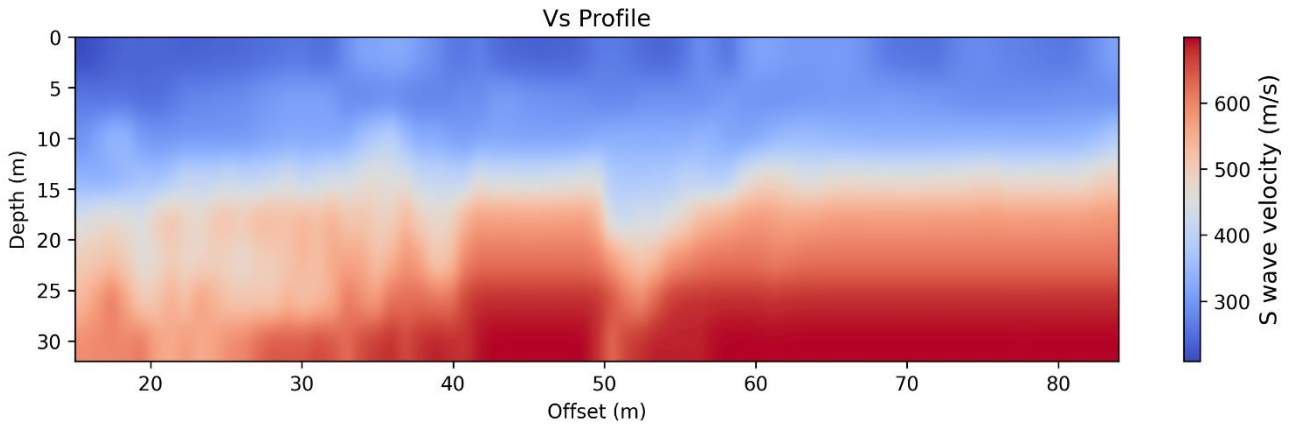

Figure 7: 2D S-wave velocity profile obtained based on one-dimensional inversion results

Proceedings DOI: 10.21467/proceedings.7.7
ISBN: 978-81-989164-3-3

Series: AIJR Proceedings
ISSN: 2582-3922

5 CONCLUSIONS AND FUTURE WORKS

5.1 Conclusions

We deployed a linear array of 48 seismic nodes at a construction site in northern Hong Kong to collect and analyze ambient noise data for nearly two days. The noise energy exhibited a marked difference between working days and rest days, demonstrating that the presence of local traffic noise and construction noise has a significant positive effect on data collection. Additionally, noise energy was slightly higher during the daytime compared to nighttime, reflecting variations in human activity across different time periods.

We investigated the effects of different stacking durations and stacking methods on the noise cross-correlation functions (NCFs). For short-term stacking (1h), employing different weighted stacking methods (SNR-weighted, PWS, tf-PWS) can effectively improve the signal-to-noise ratio of NCFs, among which PWS seems to have the best effect. For long-time stacking, even using conventional linear stacking can obtain high signal-to-noise ratio surface wave signals.

Utilizing the stacked NCFs, we extracted the dispersion curve using the phase shift method and employed the bidirectional shot mode to determine the inversion point for one-dimensional S-wave imaging. By integrating all the one-dimensional S-wave structures obtained through inversion, we built a 2D S-wave velocity profile at a depth of 30 meters in the middle part of the survey line. The velocity profile given by tomography can be combined with other engineering geophysical prospecting results such as drilling data and core data to provide useful support for engineering applications. Our results demonstrate the feasibility of shallow S-wave structural tomography based on ambient noise data in Hong Kong. It has a good application prospect in geotechnical engineering of Hong Kong and can provide reliable prior information for engineering construction and urban underground space utilization, especially considering its low cost, safety and non-intrusiveness.

5.2 Future works

In this field test, the site conditions allowed us to deploy a survey line of approximately 94 m, which posed challenges for low-frequency data acquisition and consequently limited the depth of tomography. In subsequent field tests, we will try to lay out longer survey lines in order to detect deep structural information (such as bedrock surface). In S-wave velocity structure inversion, we currently only use the fundamental mode of dispersion curve. However, some higher-order modes are visible in the surface wave dispersion spectrum (Figure 5), and we intend to incorporate them in subsequent studies to better constrain the velocity structure and enhance imaging depth. In addition, this research uses a linear node seismometer array with a station spacing of 2 m for data collection. Previous studies suggest that the inversion resolution is empirically comparable to the station spacing. By combining the current rapidly developing dense data acquisition technology (such as distributed acoustic sensing, DAS), the imaging resolution can be greatly improved. In future studies, we aim to combine node seismometers with data collected by DAS to improve the resolution of tomography.

ACKNOWLEDGEMENTS

We are very grateful to Civil Engineering and Development Department (CEDD) for providing the construction site for experiments. We thank Dr. Zhengyang Li from the Southern University of Science and Technology for helpful discussions.

REFERENCES

Aki, K., Christoffersson, A., & Husebye, E. S. (1977). Determination of the three-dimensional seismic structure of the lithosphere. *Journal of Geophysical Research*, *82*(2), 277-296.

Bensen, G. D., Ritzwoller, M. H., Barmin, M. P., Levshin, A. L., Lin, F., Moschetti, M. P., Shapiro, N. M., & Yang, Y. (2007). Processing seismic ambient noise data to obtain reliable broad-band surface wave dispersion measurements. *Geophysical Journal International*, *169*(3), 1239-1260. https://doi.org/10.1111/j.1365-246X.2007.03374.x

Brocher, T. M. (2005). Empirical relations between elastic wavespeeds and density in the Earth's crust. *Bulletin of the Seismological Society of America*, *95*(6), 2081-2092.

Buchen, P. W., & Ben-Hador, R. (1996). Free-mode surface-wave computations. *Geophysical Journal International*, *124*(3), 869-887. https://doi.org/10.1111/j.1365-246X.1996.tb05642.x

Chan, Y., Ho, K., & Pun, W. (1994). A new marble rock mass classification system for the interpretation of karst morphology in Hong Kong. *HKIE Transactions*, *1*(2), 1-12.

Cheng, F., Xia, J., Luo, Y., Xu, Z., Wang, L., Shen, C., Liu, R., Pan, Y., Mi, B., & Hu, Y. (2016). Multichannel analysis of passive surface waves based on crosscorrelations. *Geophysics*, *81*(5), EN57-EN66.

Cheng, F., Xia, J., Xu, Y., Xu, Z., & Pan, Y. (2015). A new passive seismic method based on seismic interferometry and multichannel analysis of surface waves. *Journal of Applied Geophysics*, *117*, 126-135. https://doi.org/https://doi.org/10.1016/j.jappgeo.2015.04.005

Foti, S., Parolai, S., Albarello, D., & Picozzi, M. (2011). Application of surface-wave methods for seismic site characterization. *Surveys in Geophysics*, *32*, 777-825.

Herrmann, R. B. (2013). Computer programs in seismology: An evolving tool for instruction and research. *Seismological Research Letters*, *84*(6), 1081-1088.

Kästle, E. D., Soomro, R., Weemstra, C., Boschi, L., & Meier, T. (2016). Two-receiver measurements of phase velocity: cross-validation of ambient-noise and earthquake-based observations. *Geophysical Journal International*, *207*(3), 1493-1512. https://doi.org/10.1093/gji/ggw341

Lobkis, O. I., & Weaver, R. L. (2008). On the emergence of the Green's function in the correlations of a diffuse field.

Luu, K. (2021). disba: Numba-accelerated computation of surface wave dispersion. *Zenodo, Dec*.

Nakata, N., & Snieder, R. (2012). Estimating near-surface shear wave velocities in Japan by applying seismic interferometry to KiK-net data. *Journal of Geophysical Research: Solid Earth*, *117*(B1). https://doi.org/https://doi.org/10.1029/2011JB008595

Park, C. B., Miller, R. D., & Xia, J. (1999). Multichannel analysis of surface waves. *Geophysics*, *64*(3), 800-808.

Peterson, J. R. (1993). *Observations and modeling of seismic background noise* (2331-1258).

Schimmel, M., & Paulssen, H. (1997). Noise reduction and detection of weak, coherent signals through phase-weighted stacks. *Geophysical Journal International*, *130*(2), 497-505. https://doi.org/10.1111/j.1365-246X.1997.tb05664.x

Schimmel, M., Stutzmann, E., & Gallart, J. (2011). Using instantaneous phase coherence for signal extraction from ambient noise data at a local to a global scale. *Geophysical Journal International*, *184*(1), 494-506. https://doi.org/10.1111/j.1365-246X.2010.04861.x

Sewell, R. (2000). *The pre-quaternary geology of Hong Kong*. Hong Kong Geological Survey, Geotechnical Engineering Office, Civil ….

Shapiro, N. M., Campillo, M., Stehly, L., & Ritzwoller, M. H. (2005). High-resolution surface-wave tomography from ambient seismic noise. *Science*, *307*(5715), 1615-1618. https://doi.org/10.1126/science.1108339

Van den Bergh, F., & Engelbrecht, A. P. (2004). A cooperative approach to particle swarm optimization. *IEEE transactions on evolutionary computation*, *8*(3), 225-239.

Virieux, J., & Operto, S. (2009). An overview of full-waveform inversion in exploration geophysics. *Geophysics*, *74*(6), WCC1-WCC26.

Xia, J., Miller, R. D., & Park, C. B. (1999). Estimation of near-surface shear-wave velocity by inversion of Rayleigh waves. *Geophysics*, *64*(3), 691-700.